Ann Nucl Med (2014) 28:220–226
DOI 10.1007/s12149-013-0798-1

ORIGINAL ARTICLE

Age-related decline in dopamine transporter in human brain using PET with a new radioligand [^{18}F]FE-PE2I

Yoshitoshi Shingai · Amane Tateno · Ryosuke Arakawa · Takeshi Sakayori · WooChan Kim · Hidenori Suzuki · Yoshiro Okubo

Received: 26 September 2013 / Accepted: 9 December 2013 / Published online: 3 January 2014

Abstract
Objective Dopamine transporter (DAT) density is considered as a marker of pre-synaptic function. Numerous neuroimaging studies have consistently demonstrated an age-related decrease in DAT density in normal human brain. However, the precise degree of the regional decline is not yet clear. The purpose of this study was to evaluate the effect of the normal aging process on DAT densities in human-specific brain regions including the substantia nigra and thalamus using positron emission tomography (PET) with [^{18}F]FE-PE2I, a new PET radioligand with high affinity and selectivity for DAT.
Methods Thirty-six healthy volunteers ranging in age from 22 to 80 years were scanned with PET employing [^{18}F]FE-PE2I for measuring DAT densities. Region of interest (ROI)-based analysis was used, and ROIs were manually defined for the caudate, putamen, substantia nigra, thalamus, and cerebellar cortex. DAT binding was quantified using a simplified reference tissue model, and the cerebellum was used as reference region. Estimations of binding potential in the caudate, putamen, substantia nigra, and thalamus were individually regressed according to age using simple regression analysis. Estimates of DAT loss per decade were obtained using the values from the regression slopes.
Results There were 7.6, 7.7, and 3.4 % per-decade declines in DAT in the caudate, putamen, and substantia nigra, respectively. By contrast, there was no age-related decline of DAT in the thalamus.
Conclusions [^{18}F]FE-PE2I allowed reliable quantification of DAT, not only in the caudate and putamen but also in the substantia nigra. From the results, we demonstrated the age-related decline in the caudate and putamen as reported in previous studies, and additionally for those in the substantia nigra for the first time.

Keywords [^{18}F]FE-PE2I · Human · Positron emission tomography (PET) · Dopamine transporter (DAT) · Aging

Y. Shingai · A. Tateno · R. Arakawa · T. Sakayori · W. Kim · Y. Okubo (✉)
Department of Neuropsychiatry, Nippon Medical School, Sendagi 1-1-5, Bunkyo-ku, Tokyo 113-8602, Japan
e-mail: okubo-y@nms.ac.jp

R. Arakawa
Department of Adult Mental Health, National Institute of Mental Health, National Center of Neurology and Psychiatry, Tokyo, Japan

H. Suzuki
Department of Pharmacology, Nippon Medical School, Tokyo, Japan

Introduction

Dopamine transporter (DAT) plays a crucial role in the regulation of dopamine concentration in the synaptic cleft by dopamine reuptake, and its density is considered as a marker of pre-synaptic function. Changes in the density and function of DAT in living human brain have been reported in studies of various neuropsychiatric disorders using PET, such as Parkinson's disease (PD) [1–3], Huntington's disease [4], attention-deficit/hyperactivity disorder [5], autism [6], and schizophrenia [7]. Further, several in vivo PET studies [2, 8–13] and in vitro neurobiological studies [14–18] have consistently demonstrated a significant age-related decrease of DAT in the striatum.

A number of radioligands for imaging DAT have been developed: [^{11}C]Cocaine [19], [^{11}C]CFT [20], [^{11}C]β-CIT [21], [^{11}C]MP [22], [^{18}F]CFT [23], [^{18}F]FPCIT [2],

[^{18}F]FECNT [24], and [^{11}C]PE2I [25]. But their low affinity for DAT, poor selectivity for other monoamine transporters, impossibility to reach peak uptake in the striatum due to slow kinetics, and production of radiometabolites that could potentially permeate the blood–brain barrier have been argued.

Recently, a fluoroethyl analog of PE2I, ^{18}F-(E)-*N*-(3-iodoprop-2E-enyl)-2β-carbofluoroethoxy-3β-(4-methylphenyl)nortropane ([^{18}F]FE-PE2I), was developed [26]. [^{18}F]FE-PE2I showed high affinity and high selectivity for DAT, fast kinetics and low production of BBB-permeable radiometabolites. From these characteristics, [^{18}F]FE-PE2I appears to be the most promising radioligand for quantifying DAT in humans not only in the striatum but also in lower binding regions such as the substantia nigra and thalamus.

In this study, we aimed to investigate the effect of the normal aging process on DAT in living human-specific brain regions including the substantia nigra and thalamus using PET with a new radioligand, [^{18}F]FE-PE2I.

Materials and methods

Subjects

Thirty-six healthy volunteers aged 22–80 years (mean ± SD 48.5 ± 19.1; 8 subjects between 20 and 29, 7 between 30 and 39, 6 between 40 and 49, 0 between 50 and 59, 7 between 60 and 69, 7 between 70 and 79, 1 between 80 and 89; 15 women and 21 men) were enrolled in the study. None had a history of present or past psychiatric, neurological, or somatic disorders, alcohol- or drug-related problems. All subjects were non-smokers. The study was approved by the ethics committee and review board of Nippon Medical School Hospital, Tokyo, Japan. After thorough explanation of the study, written informed consent was obtained from all participants.

PET procedures

[^{18}F]FE-PE2I was synthesized from its precursor, tosylethyl-PE2I, through nucleophilic fluorination reaction. PET scans were carried out with an Eminence SET-3000GCT-X (Shimadzu Corp., Kyoto, Japan) scanner to measure regional brain radioactivity. This scanner provides 99 sections with an axial field of view (FOV) of 26.0 cm. The spatial resolution was 3.45 mm in-plane and 3.72 mm full-width at half-maximum (FWHM) axially. A head fixation device was used during the scans. A 10-min transmission scan using a ^{137}Cs line source was done to correct for attenuation. Dynamic PET scan was performed for 60 min (20 s × 9, 1 min × 5, 2 min × 4, 4 min × 11) after intravenous bolus injection of [^{18}F]FE-PE2I. Injected radioactivity was 175.0–191.1 (mean ± SD 185.7 ± 3.7) MBq, and specific radioactivity was 90.0–307.6 (174.4 ± 61.4) GBq/μmol.

MRI procedures

Magnetic resonance (MR) images of the brain were acquired with 1.5 T MR imaging, Intera 1.5 T Achieve Nova (Philips Medical Systems, Best, Netherlands). T1-weighted MR images were obtained at 1-mm slices. The MR images revealed no brain abnormalities in the subjects and were used as reference for drawing regions of interest (ROIs) on PET images.

Data analysis

All MR images were coregistered to the PET images using PMOD (version 3.3; PMOD Technologies Ltd., Zurich, Switzerland). ROIs were drawn manually on overlaid summated PET and coregistered MR images of each subject using PMOD. ROIs were defined for the caudate, putamen, substantia nigra, thalamus and cerebellar cortex (Fig. 1). Because of the difficulty of defining the substantia nigra on MR images, we drew ROIs of almost the same shape and size in all subjects to contain the most intense activity in each slice on the summated PET images. The accuracy of the setting was verified twice by different persons. The average values of right and left ROIs were used for the analysis. The data were not subjected to motion correction. DAT binding was quantified using a simplified reference tissue model (SRTM) [27, 28]. The cerebellum was used as reference region because of its negligible DAT density [29]. These models allow the estimation of binding potential (BP_{ND}), which was defined as $f_{ND} \times B_{max}/K_d$, where f_{ND} is the free fraction of ligand in the non-displaceable tissue compartment, B_{max} is the transporter density, and K_d is the dissociation constant [30].

Statistical analysis

BP_{ND}s for [^{18}F]FE-PE2I in the caudate, putamen, substantia nigra, and thalamus were individually regressed by age using simple regression analysis. Regression analyses in these four regions were also performed separately in men and women. Estimates of DAT loss per decade, as assessed by BP_{ND}s for [^{18}F]FE-PE2I, were obtained using the values from the regression slopes. In all tests, a P value of <0.05 was considered statistically significant. The statistical computations were performed using the software package, SPSS Statistics 21 (IBM Corp., NY, USA).

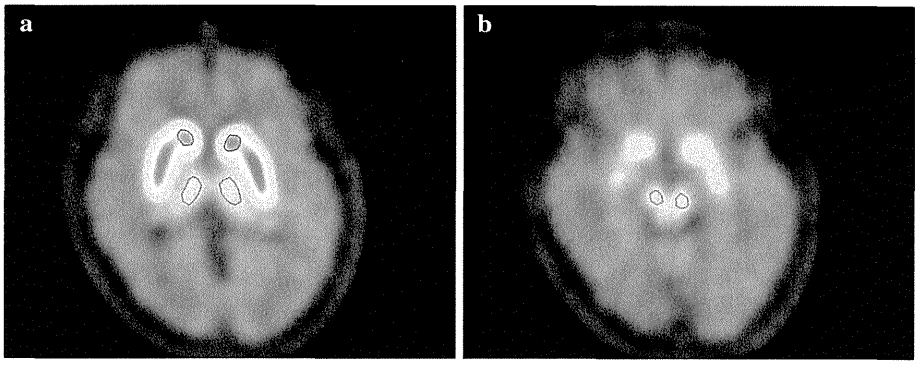

Fig. 1 Summated images of [^{18}F]FE-PE2I with regions of interest. One subject is shown at the level of the caudate, putamen, thalamus (a), and the substantia nigra (b)

Table 1 Demographics of the 36 normal individuals assessed

Region	BP_{ND}		Change per decade (%)	P value
	Range	Mean ± SD		
Caudate	1.65–4.08	2.84 ± 0.54	−7.6	<0.0001
Putamen	1.79–4.31	3.07 ± 0.58	−7.7	<0.0001
Substantia nigra	0.31–0.74	0.52 ± 0.09	−3.4	<0.05
Thalamus	0.2–0.56	0.37 ± 0.08	None	None

BP_{ND} binding potential

Results

The mean BP_{ND} values estimated by the SRTM method for [^{18}F]FE-PE2I were 2.84, 3.07, 0.52, and 0.37 in the caudate, putamen, substantia nigra, and thalamus, respectively, with ranges of 1.65–4.08, 1.79–4.31, 0.31–0.74, and 0.2–0.56 (Table 1). Simple correlation analysis showed an inverse relationship between BP_{ND} and age in the caudate ($r = -0.84$, $P < 0.0001$), putamen ($r = -0.85$, $P < 0.0001$), and substantia nigra ($r = -0.39$, $P < 0.05$) (Fig. 2a–c). This age-related decline corresponded to 7.6, 7.7, and 3.4 % reduction per decade in the caudate, putamen, and substantia nigra, respectively (Table 1). In contrast, there was no age-related decline in the thalamus ($r = -0.11$, $P = 0.52$) (Fig. 2d).

Age-related decline of BP_{ND} in the caudate and putamen were observed in both men ($r = -0.88$, $P < 0.0001$ and $r = -0.89$, $P < 0.0001$) and women ($r = -0.8$, $P < 0.0004$ and $r = -0.83$, $P < 0.0002$). By contrast, in the substantia nigra, age-related decline of BP_{ND} was observed in men ($r = -0.57$, $P < 0.008$), but it was not seen in women ($r = -0.24$, $P = 0.38$). In the thalamus, age-related decline of BP_{ND} was not observed in either men or women ($r = -0.3$, $P = 0.18$ and $r = 0.11$, $P = 0.69$).

Discussion

In the present study, DAT function was assessed in normal individual human brain over a wide age range. The main finding was an age-related decline of [^{18}F]FE-PE2I BP_{ND} in the caudate and putamen, as was reported in previous studies. In addition, a decline in the substantia nigra was demonstrated for the first time, but, interestingly, in men only.

This is the first PET study of the effect of normal aging process on DAT function in living human brain using [^{18}F]FE-PE2I. Previous PET studies of the association of age-related changes with DAT have been performed using [^{11}C]Cocaine [11], [^{11}C]D-threo-methylphenidate [10, 12], [^{18}F]FPCIT [2], [^{11}C]β-CFT [9], and [^{11}C]CFT [8]. Most of these radioligands are analogs of cocaine and have a rather low affinity for DAT. Furthermore, they have measurable affinity for serotonin transporter (SERT) and norepinephrine transporter (NET), reflecting the poor selectivity for DAT [31] (Table 2). For example, cocaine showed relatively low affinity for DAT (inhibition constant, $K_i = 350$ nM) and had affinity for other monoamine transporters such as SERT ($Ki = 1{,}500$ nM) and NET ($K_i = 1{,}500$ nM), indicating low selectivity.

PE2I has high affinity and good selectivity for DAT ($K_i = 17$ nM for DAT, 500 nM for SERT, and >1,000 nM for NET) [32]. [^{11}C]PE2I has been utilized for DAT quantification in several human PET studies [33–35]. However, there were some problems quantifying DAT with [^{11}C]PE2I because of its slow kinetics properties in the striatum, where BP_{ND} values are severely underestimated (~50 %) by the reference tissue method [33, 36]. In addition, at least one radiometabolite of [^{11}C]PE2I has been found to cross the blood–brain barrier (BBB) in rats, potentially interfering with DAT quantification [37].

[^{18}F]FE-PE2I was then developed [26] to solve these problems. It showed high affinity for DAT ($K_i = 12$ nM), almost the same as [^{11}C]PE2I. On the other hand, because of its fast kinetics, quantification with 60 min was possible

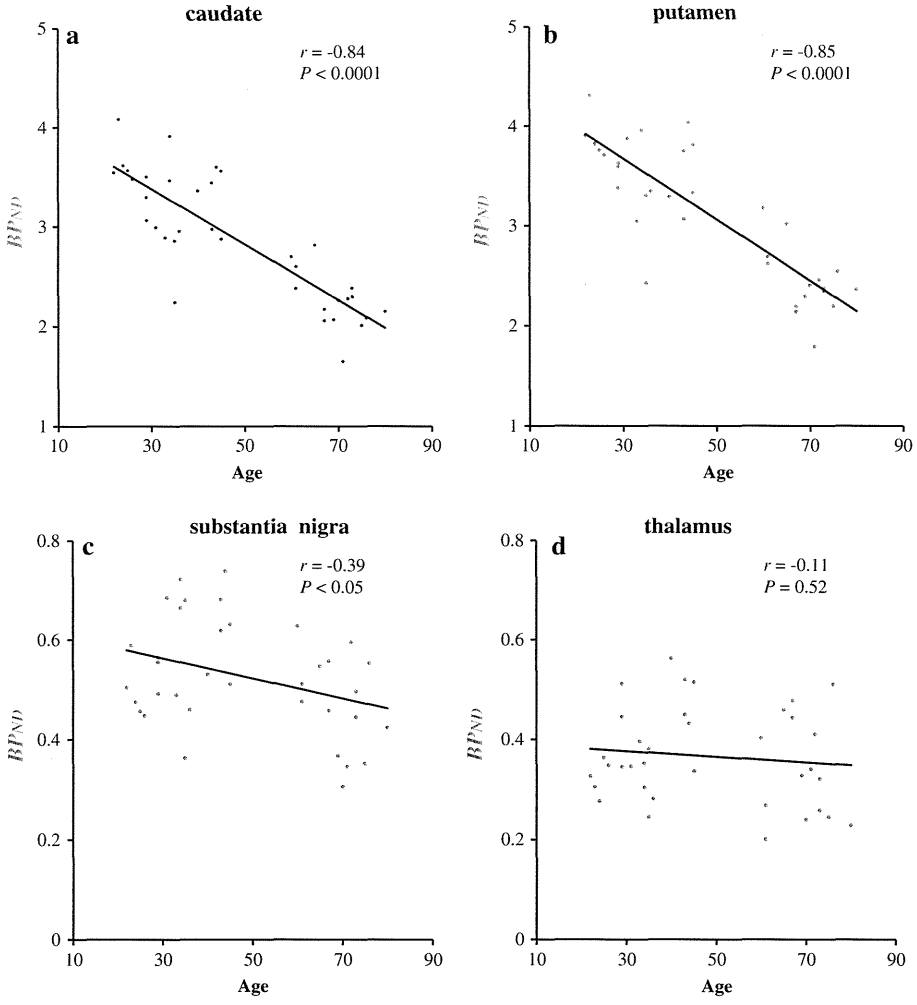

Fig. 2 Results of simple correlation analysis between age and BP_{ND} for [^{18}F]FE-PE2I in the caudate (a), putamen (b), substantia nigra (c), and thalamus (d)

Table 2 Affinities for monoamine transporter of ligands in evaluating age-related changes of dopamine transporter (DAT)

Ligand	Affinity (K_i, nM)		
	DAT	SERT	NET
Cocaine	350	1,500	1,500
D-Threo-methylphenidate	54.3	>10,000	126
FP-CIT	3.53	1.68	63
CFT	14.7	181	635
FE-PE2I	12	>1,000	None[a]

[a] NET inhibitor maprotiline showed no effect in autographic and PET studies [26]

and the SRTM method yielded less biased BP_{ND} than [^{11}C]PE2I. Additionally, the effect of radiometabolites of [^{18}F]FE-PE2I on quantification was likely to be small [29]. These characteristics allowed reliable quantification of specific binding not only in the striatum but also in lower binding regions such as the substantia nigra and thalamus. Thus, [^{18}F]FE-PE2I could be the most reliable and accurate radioligand for the regional quantification of DAT.

In the ROI-based analysis, DAT density measured by [^{18}F]FE-PE2I was lost at rates of 7.6 and 7.7 % per decade in the caudate and putamen, respectively. These results were comparable to previous in vivo human PET studies that showed a linear decline in DAT density ranging from 4.4 to 11.2 % per decade. Factors in demographics such as subject numbers (7–33 subjects) and the distribution of subjects per age range may have caused the decreasing rate differences in previous studies [2, 8–13] (Table 3). In the present study, the decline rate per decade of DAT density in the caudate and putamen were measured by [^{18}F]FE-PE2I, the most reliable radioligand for DAT. Furthermore, the number of subjects (36) and wide age range (22–80 years) in our data were more than those of the previous studies. Therefore, we think that the DAT decline rates per decade (7.6 and 7.7 % in the caudate and putamen, respectively) in our study are the most reliable values.

In the substantia nigra, DAT density was lost at a rate of 3.4 % per decade, but no comparable in vivo human data

Table 3 In vivo human PET data: age-related changes of dopamine transporter (DAT)

References	Ligand	n	Age range (years)	Change per decade (%)	Region
Volkow et al. [11]	[^{11}C]Cocaine	26	21–63	−7.0	Striatum
Volkow et al. [12]	[^{11}C]D-threo-methylphenidate	23	20–74	−6.6	Striatum
Kazumata et al. [2]	[^{18}F]FPCIT	7	23–73	−7.7	Caudate
				−6.4	Putamen
Rinne et al. [9]	[^{11}C]β-CFT	15	23–70	−4.7	Caudate
				−4.4	Putamen
Volkow et al. [13]	[^{11}C]D-threo-methylphenidate	21	24–86	−5[a]	Striatum
Ishibashi et al. [8]	[^{11}C]CFT	16	21–74	−6.1	Caudate
				−5.5	Anterior putamen
				−5.6	Posterior putamen
Troiano et al. [10]	[^{11}C]D-threo-methylphenidate	33	27–77	−11.2	Caudate
				−10.5	Putamen
Present data	[^{18}F]FE-PE2I	36	22–80	−7.6	Caudate
				−7.7	Putamen
				−3.4	Substantia nigra

[a] Estimated by the chart in original article

were reported. Because of less specific to non-displaceable binding ratio and selectivity for DAT, previous DAT ligands could not evaluate DAT density in the midbrain. In the study of post-mortem human brain, it was confirmed that dopaminergic neuronal loss occurs in the substantia nigra [38, 39]. In 36 control cases (21–90 years), the total neuronal count fell 4.7 % per decade in the pars compacta [38]. And, in 62 control cases (40–90 years), the total neuronal count fell 4.7–6.0 % in the substantia nigra. If based on the hypothesis that neuronal cell loss reflects a decrease in DAT, our results were comparable to previous post-mortem human brain studies. Because our result is the first in vivo human data at present, and there were also no major differences in comparison with the degree of neuronal cell loss in previous post-mortem studies, the age-related decline of DAT density in the substantia nigra was considered to be fairly accurate at 3.4 % per decade.

In human brain, dopaminergic neurons in the substantia nigra pars compacta project particularly to the striatum. In this regard, the loss of dopamine neurons in the substantia nigra and the reduction of dopaminergic projection to the striatum are considered to represent the pathology of PD. Post-mortem studies of patients with PD demonstrated severe reduction in dopamine neurons especially in the putamen [40].

Previous in vivo neuroimaging studies showed gender differences in the dopaminergic system [41]. In our study, age-related decline of DAT density in the substantia nigra was observed in men ($r = -0.57$, $P < 0.008$) but not in women ($r = -0.24$, $P = 0.38$). The incidence of PD is known to be greater in men than in women [41, 42]. Additionally, gender differences in the clinical symptoms of PD were reported [42]. These features concerning PD may be related to the gender differences of the age-related decline of DAT density reported in our study. The in vivo assessment of the substantia nigra or subdivisions of the striatum using [^{18}F]FE-PE2I, considering the gender differences, might allow us further understanding of the pathology of PD.

In the thalamus, there was no age-related decline of DAT density ($r = -0.11$, $P = 0.52$). Although we could measure DAT density in the thalamus with [^{18}F]FE-PE2I, BP_{ND} values were approximately 0.4, much less than in the caudate and putamen. We may fail to detect the age-related decline of DAT because of such low BP_{ND} values. Another possible reason is that there might be no age-related change in DAT in the thalamus originally. Further studies both in vitro and in vivo concerning age-related DAT change in the thalamus will be needed to clarify this point.

There are some limitations to this study. First, because the volume of the substantia nigra is small, a partial volume effect should be considered. However, Hagemeier et al. [43] reported that there was no age-related volume reduction in the substantia nigra. Furthermore, we drew ROIs of almost the same shape and size in all subjects to contain the most intense activity in each slice on the summated PET images. Based on these factors, the influence of the partial volume effect in the substantia nigra may be assumed to be minimal. Second, because it was conducted by cross-sectional studies in each subject, the same as previously reported, it is clear that the differences between subjects can affect the results of interpreting the effects of aging. Furthermore, the absence of subjects in the 50–59 year age range may handicap the accurate assessment of the age-

related decline rate of DAT per decade. Longitudinal studies with larger study populations will allow more accurate quantification of the age-related decline rate of DAT throughout the human life span.

Conclusions

In this study, we demonstrated an age-related decline of [^{18}F]FE-PE2I BP_{ND} in several brain regions, and especially in the substantia nigra. [^{18}F]FE-PE2I enables us to compare regional distributions of DAT binding, and it can also be used in the investigation of neuropsychiatric disorders related to DAT density, function and aging effect.

Acknowledgments The authors thank Dr. Kiichi Ishiwata (Positron Medical Center, Tokyo Metropolitan Institute of Gerontology, Tokyo, Japan) and Dr. Shinji Kageyama (Mitsubishi Chemical Medience Corp., Tokyo, Japan), Mr. Koji Nagaya, Mr. Koji Kanaya, Mr. Masaya Suda, Ms. Megumi Takei, Mr. Kazuyoshi Honjo, and Mr. Minoru Sakurai (Clinical Imaging Center for Healthcare, Nippon Medical School, Tokyo, Japan) for their assistance with this study. This work was partially supported by a grant from the Ministry of Education, Culture, Sports, Science and Technology (MEXT, Japan). Dr. Suzuki has received speaker's honoraria from Pfizer and Eisai within the past 3 years. Dr. Okubo has received grants or speaker's honoraria from Dainippon Sumitomo Pharma, GlaxoSmithKline, Janssen Pharmaceutical, Otsuka, Pfizer, Eli Lilly, Astellas, Yoshitomi and Meiji within the past 3 years. For the remaining authors none were declared.

References

1. Chou KL, Bohnen NI. Performance on an Alzheimer-selective odor identification test in patients with Parkinson's disease and its relationship with cerebral dopamine transporter activity. Parkinsonism Relat Disord. 2009;15(9):640–3.
2. Kazumata K, Dhawan V, Chaly T, Antonini A, Margouleff C, Belakhlef A, et al. Dopamine transporter imaging with fluorine-18-FPCIT and PET. J Nucl Med. 1998;39(9):1521–30.
3. Oh M, Kim JS, Kim JY, Shin K-H, Park SH, Kim HO, et al. Subregional patterns of preferential striatal dopamine transporter loss differ in Parkinson disease, progressive supranuclear palsy, and multiple-system atrophy. J Nucl Med. 2012;53(3):399–406.
4. Ginovart N, Lundin A, Farde L, Halldin C, Bäckman L, Swahn CG, et al. PET study of the pre- and post-synaptic dopaminergic markers for the neurodegenerative process in Huntington's disease. Brain. 1997;120(Pt 3):503–14.
5. Jucaite A, Fernell E, Halldin C, Forssberg H, Farde L. Reduced midbrain dopamine transporter binding in male adolescents with attention-deficit/hyperactivity disorder: association between striatal dopamine markers and motor hyperactivity. Biol Psychiatry. 2005;57(3):229–38.
6. Nakamura K, Sekine Y, Ouchi Y, Tsujii M, Yoshikawa E, Futatsubashi M, et al. Brain serotonin and dopamine transporter bindings in adults with high-functioning autism. Arch Gen Psychiatry. 2010;67(1):59–68.
7. Arakawa R, Ichimiya T, Ito H, Takano A, Okumura M, Takahashi H, et al. Increase in thalamic binding of [(11)C]PE2I in patients with schizophrenia: a positron emission tomography study of dopamine transporter. J Psychiatr Res. 2009;43(15):1219–23.
8. Ishibashi K, Ishii K, Oda K, Kawasaki K, Mizusawa H, Ishiwata K. Regional analysis of age-related decline in dopamine transporters and dopamine D2-like receptors in human striatum. Synapse. 2009;63(4):282–90.
9. Rinne JO, Sahlberg N, Ruottinen H, Någren K, Lehikoinen P. Striatal uptake of the dopamine reuptake ligand [11C]beta-CFT is reduced in Alzheimer's disease assessed by positron emission tomography. Neurology. 1998;50(1):152–6.
10. Troiano AR, Schulzer M, de la Fuente-Fernandez R, Mak E, McKenzie J, Sossi V, et al. Dopamine transporter PET in normal aging: dopamine transporter decline and its possible role in preservation of motor function. Synapse. 2010;64(2):146–51.
11. Volkow ND, Fowler JS, Wang GJ, Logan J, Schlyer D, MacGregor R, et al. Decreased dopamine transporters with age in health human subjects. Ann Neurol. 1994;36(2):237–9.
12. Volkow ND, Ding YS, Fowler JS, Wang GJ, Logan J, Gatley SJ, et al. Dopamine transporters decrease with age. J Nucl Med. 1996;37(4):554–9.
13. Volkow ND, Wang GJ, Fowler JS, Ding YS, Gur RC, Gatley J, et al. Parallel loss of presynaptic and postsynaptic dopamine markers in normal aging. Ann Neurol. 1998;44(1):143–7.
14. Allard P, Marcusson JO. Age-correlated loss of dopamine uptake sites labeled with [3H]GBR-12935 in human putamen. Neurobiol Aging. 1989;10(6):661–4.
15. De Keyser J, Ebinger G, Vauquelin G. Age-related changes in the human nigrostriatal dopaminergic system. Ann Neurol. 1990;27(2):157–61.
16. Emborg ME, Ma SY, Mufson EJ, Levey AI, Taylor MD, Brown WD, et al. Age-related declines in nigral neuronal function correlate with motor impairments in rhesus monkeys. J Comp Neurol. 1998;401(2):253–65.
17. Hebert MA, Larson GA, Zahniser NR, Gerhardt GA. Age-related reductions in [3H]WIN 35,428 binding to the dopamine transporter in nigrostriatal and mesolimbic brain regions of the fischer 344 rat. J Pharmacol Exp Ther. 1999;288(3):1334–9.
18. Zelnik N, Angel I, Paul SM, Kleinman JE. Decreased density of human striatal dopamine uptake sites with age. Eur J Pharmacol. 1986;126(1–2):175–6.
19. Fowler JS, Volkow ND, Wolf AP, Dewey SL, Schlyer DJ, Macgregor RR, et al. Mapping cocaine binding sites in human and baboon brain in vivo. Synapse. 1989;4(4):371–7.
20. Wong DF, Yung B, Dannals RF, Shaya EK, Ravert HT, Chen CA, et al. In vivo imaging of baboon and human dopamine transporters by positron emission tomography using [11C]WIN 35,428. Synapse. 1993;15(2):130–42.
21. Farde L, Halldin C, Müller L, Suhara T, Karlsson P, Hall H. PET study of [11C]beta-CIT binding to monoamine transporters in the monkey and human brain. Synapse. 1994;16(2):93–103.
22. Ding YS, Fowler JS, Volkow ND, Gatley SJ, Logan J, Dewey SL, et al. Pharmacokinetics and in vivo specificity of [11C]dl-threo-methylphenidate for the presynaptic dopaminergic neuron. Synapse. 1994;18(2):152–60.
23. Laakso A, Bergman J, Haaparanta M, Vilkman H, Solin O, Hietala J. [18F]CFT [(18F)WIN 35,428], a radioligand to study the dopamine transporter with PET: characterization in human subjects. Synapse. 1998;28(3):244–50.
24. Davis MR, Votaw JR, Bremner JD, Byas-Smith MG, Faber TL, Voll RJ, et al. Initial human PET imaging studies with the dopamine transporter ligand 18F-FECNT. J Nucl Med. 2003;44(6):855–61.
25. Halldin C, Erixon-Lindroth N, Pauli S, Chou Y-H, Okubo Y, Karlsson P, et al. [(11)C]PE2I: a highly selective radioligand for PET examination of the dopamine transporter in monkey and human brain. Eur J Nucl Med Mol Imaging. 2003;30(9):1220–30.

26. Varrone A, Steiger C, Schou M, Takano A, Finnema SJ, Guilloteau D, et al. In vitro autoradiography and in vivo evaluation in cynomolgus monkey of [18F]FE-PE2I, a new dopamine transporter PET radioligand. Synapse. 2009;63(10):871–80.
27. Ito H, Sudo Y, Suhara T, Okubo Y, Halldin C, Farde L. Error analysis for quantification of [(11)C]FLB 457 binding to extrastriatal D(2) dopamine receptors in the human brain. Neuroimage. 2001;13(3):531–9.
28. Lammertsma AA, Hume SP. Simplified reference tissue model for PET receptor studies. Neuroimage. 1996;4(3 Pt 1):153–8.
29. Sasaki T, Ito H, Kimura Y, Arakawa R, Takano H, Seki C, et al. Quantification of dopamine transporter in human brain using PET with 18F-FE-PE2I. J Nucl Med. 2012;53(7):1065–73.
30. Innis RB, Cunningham VJ, Delforge J, Fujita M, Gjedde A, Gunn RN, et al. Consensus nomenclature for in vivo imaging of reversibly binding radioligands. J Cereb Blood Flow Metab. 2007;27(9):1533–9.
31. Kula NS, Baldessarini RJ, Tarazi FI, Fisser R, Wang S, Trometer J, et al. [3H]beta-CIT: a radioligand for dopamine transporters in rat brain tissue. Eur J Pharmacol. 1999;385(2–3):291–4.
32. Emond P, Garreau L, Chalon S, Boazi M, Caillet M, Bricard J, et al. Synthesis and ligand binding of nortropane derivatives: N-substituted 2beta-carbomethoxy-3beta-(4′-iodophenyl)nortropane and N-(3-iodoprop-(2E)-enyl)-2beta-carbomethoxy-3beta-(3′,4′-disubstituted phenyl)nortropane. New high-affinity and selective compound. J Med Chem. 1997;40(9):1366–72.
33. Jucaite A, Odano I, Olsson H, Pauli S, Halldin C, Farde L. Quantitative analyses of regional [11C]PE2I binding to the dopamine transporter in the human brain: a PET study. Eur J Nucl Med Mol Imaging. 2006;33(6):657–68.
34. Odano I, Varrone A, Savic I, Ciumas C, Karlsson P, Jucaite A, et al. Quantitative PET analyses of regional [11C]PE2I binding to the dopamine transporter—application to juvenile myoclonic epilepsy. Neuroimage. 2012;59(4):3582–93.
35. Seki C, Ito H, Ichimiya T, Arakawa R, Ikoma Y, Shidahara M, et al. Quantitative analysis of dopamine transporters in human brain using [11C]PE2I and positron emission tomography: evaluation of reference tissue models. Ann Nucl Med. 2010;24(4):249–60.
36. Hirvonen J, Johansson J, Teräs M, Oikonen V, Lumme V, Virsu P, et al. Measurement of striatal and extrastriatal dopamine transporter binding with high-resolution PET and [11C]PE2I: quantitative modeling and test–retest reproducibility. J Cereb Blood Flow Metab. 2008;28(5):1059–69.
37. Shetty HU, Zoghbi SS, Liow J-S, Ichise M, Hong J, Musachio JL, et al. Identification and regional distribution in rat brain of radiometabolites of the dopamine transporter PET radioligand [11C]PE2I. Eur J Nucl Med Mol Imaging. 2007;34(5):667–78.
38. Fearnley JM, Lees AJ. Ageing and Parkinson's disease: substantia nigra regional selectivity. Brain. 1991;114(Pt 5):2283–301.
39. Gibb WR, Lees AJ. Anatomy, pigmentation, ventral and dorsal subpopulations of the substantia nigra, and differential cell death in Parkinson's disease. J Neurol Neurosurg Psychiatry. 1991;54(5):388–96.
40. Kish SJ, Shannak K, Hornykiewicz O. Uneven pattern of dopamine loss in the striatum of patients with idiopathic Parkinson's disease. Pathophysiologic and clinical implications. N Engl J Med. 1988;318(14):876–80.
41. Cosgrove KP, Mazure CM, Staley JK. Evolving knowledge of sex differences in brain structure, function, and chemistry. Biol Psychiatry. 2007;62(8):847–55.
42. Miller IN, Cronin-Golomb A. Gender differences in Parkinson's disease: clinical characteristics and cognition. Mov Disord. 2010;25(16):2695–703.
43. Hagemeier J, Dwyer MG, Bergsland N, Schweser F, Magnano CR, Heininen-Brown M, et al. Effect of age on MRI phase behavior in the subcortical deep gray matter of healthy individuals. AJNR Am J Neuroradiol. 2013;34:2144–51.

—Photogravure—

Amyloid Positron Emission Tomography Imaging for the Differential Diagnosis of Alzheimer's Disease

Amane Tateno, Takeshi Sakayori and Yoshiro Okubo
Department of Neuropsychiatry, Graduate School of Medicine, Nippon Medical School

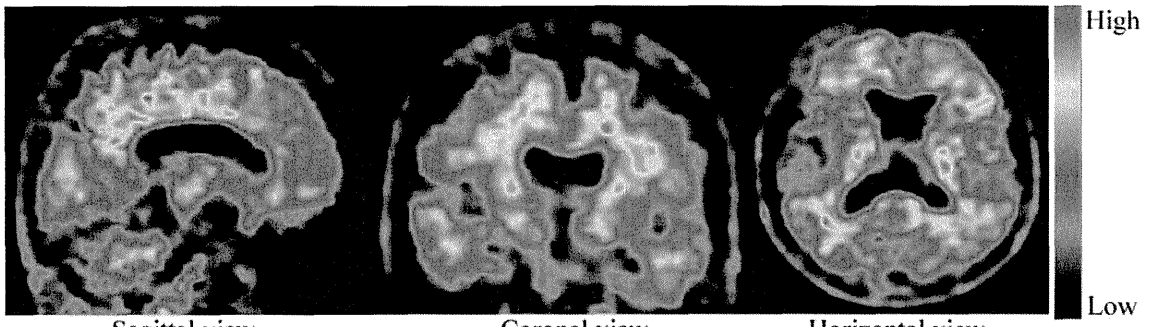

Fig. 1

On the basis of the beta-amyloid cascade theory of Alzheimer's disease (AD), in which beta-amyloid leads to the neurodegeneration that triggers the course of AD, the early detection of beta-amyloid has become important for the diagnosis of AD. In April 2012, the U.S. Food and Drug Administration approved [^{18}F]florbetapir[1], a positron emission tomography (PET) ligand, for the differential diagnosis of other types of dementia from AD[2]. Unfortunately, [^{18}F]florbetapir has not yet been approved by Japan's Pharmaceutical and Medical Devices Agency, although we have been performing amyloid PET studies with [^{18}F]florbetapir since April 2010.

Here we present amyloid PET images produced with [^{18}F]florbetapir. Both patients were suspected of having AD on the basis of their symptoms. Patient A was a 71-year-old woman with cognitive impairment (Mini-Mental State Examination [MMSE][3] score of 23). Because magnetic resonance imaging (MRI) of the brain showed no abnormality, and morphometrical analysis with the Voxel-based Specific Regional analysis system for Alzheimer's Disease (VSRAD)[4] showed no significant atrophic changes in the hippocampus (z-score, 0.97), she was suspected of having early AD. Then, PET was performed to examine amyloid accumulation (**Fig. 1**). The result of amyloid PET for patient A was interpreted as being positive for beta-amyloid. The diagnosis of AD was based on the combination of symptoms and the results of amyloid PET imaging. During follow-up the patient's cognitive performance gradually declined.

Patient B was a 74-year-old woman with depression and cognitive impairment (MMSE of 24). Brain MRI showed no abnormality. The Geriatric Depression Scale score was 13. The atrophic changes in the hippocampus were evaluated with MRI and VSRAD (z-score 1.04). She was also suspected of having early AD, and amyloid PET was performed (**Fig. 2**). In contrast to those in patient A, the results of amyloid PET in patient B ruled out the possibility of AD, and depression was diagnosed. After a 1 month of treatment, her cognitive performance had improved (MMSE of 29).

Beta-amyloid appears to accumulate gradually over 10 to 20 years before symptoms of dementia appear[5]. The increased levels of accumulated beta-amyloid detected with [^{18}F]florbetapir might be a marker of preclinical AD[6]. Although the clinical symptoms of patient B were similar to those of patient A, amyloid PET indicated that

Correspondence to Amane Tateno, Department of Neuropsychiatry, Graduate School of Medicine, Nippon Medical School, 1-1-5 Sendagi, Bunkyo-ku, Tokyo 113-8603, Japan

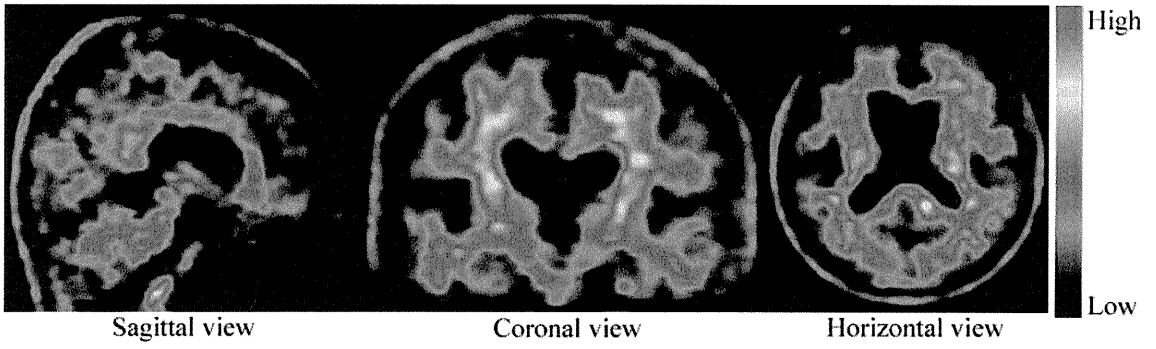

Fig. 2

patient A had early AD, whereas patient B did not. Amyloid PET imaging, as a biomarker of AD, was useful for the differential diagnosis of AD. Amyloid PET imaging might be used to predict the treatment outcome based on the amyloid pathology.

Fig. 1 PET images from patient A. The degree of beta-amyloid accumulation was visualized with color-coded scale. These images show the significant increase in beta-amyloid accumulation in the medial orbital frontal, temporal, anterior, and pesterior cingulate, and parietal lobes and the precuneus. Visual assessment by means of global rating assessment was grade 3 (moderate to high), which is defined as "nearly all cortical areas show clearly increased activity compared with the cerebellum, and most cortical regions have activity similar to the activity in white matter."

Fig. 2 PET images from patient B. The degree of beta-amyloid accumulation was visualized with color-coded scale. These images do not show the significant increase of beta-amyloid accumulation in cortical regions. Visual assessment by means of global rating assessment was grade 0 (none), which is defined as "no definite increased cortical gray matter retention of compound above cerebellum levels is present, white matter activity is clearly greater than cortical activity, and a characteristic white matter pattern is seen."

References

1. Zhang W, Oya S, Kung MP, et al.: F-18 stilbenes as PET imaging agents for detecting beta-amyloid plaques in the brain. J Med Chem 2005; 48: 5980–5988.
2. Yang L, Rieves D, Ganley C: Brain amyloid imaging - FDA approval of florbetapir F18 injection. N Engl J Med 2012; 367: 885–887.
3. Folstein MF, Folstein SE, McHugh PR: "Mini-mental state". A practical method for grading the cognitive state of patients for the clinician. J Psychiatr Res 1975; 12: 189–198.
4. Matsuda H, Mizumura S, Nemoto K, et al.: Automatic voxel-based morphometry of structural MRI by SPM8 plus diffeomorphic anatomic registration through exponentiated Lie algebra improves the diagnosis of probable Alzheimer disease. AJNR Am J Neuroradiol 2012; 33: 1109–1114.
5. Jack CR Jr, Lowe VJ, Weigand SD, et al.: Serial PiB and MRI in normal, mild cognitive impairment and Alzheimer's disease: implications for sequence of pathological events in Alzheimer's disease. Brain 2009; 132: 1355–1365.
6. Rosenberg PG, Wong DF, Edell SL, et al.: Cognition and amyloid load in Alzheimer disease imaged with florbetapir F 18 (AV-45) positron emission tomography. Am J Geriatr Psychiatry 2013; 21: 272–278.

E-mail: amtateno@nms.ac.jp Journal Website (http://www.nms.ac.jp/jnms/)

Original article

Nuclear Medicine Communications

Reproducibility of PET measurement for presynaptic dopaminergic functions using L-[β-^{11}C]DOPA and [^{18}F]FE-PE2I in humans

Masayuki Suzuki[a,d], Hiroshi Ito[b], Fumitoshi Kodaka[a], Harumasa Takano[a], Yasuyuki Kimura[a], Hironobu Fujiwara[a], Takeshi Sasaki[a], Keisuke Takahata[a], Tsuyoshi Nogami[a], Tomohisa Nagashima[a], Nobuki Nengaki[c], Kazunori Kawamura[c], Ming-Rong Zhang[c], Andrea Varrone[e], Christer Halldin[e], Yoshiro Okubo[d] and Tetsuya Suhara[a]

Objective **Recent PET studies have indicated altered presynaptic function and relation with psychotic symptoms in patients with schizophrenia. The L-[β-^{11}C]DOPA uptake rate reflects the dopamine synthesis capacity (k_{ref}), whereas the nondisplaceable binding potential (BP_{ND}) of [^{18}F]FE-PE2I reflects the dopamine transporter availability. Although the k_{ref} values of L-[β-^{11}C]DOPA and the BP_{ND} of [^{18}F]FE-PE2I can be potential markers for evaluating the severity of positive symptoms, test–retest reproducibility has not been confirmed. The purpose of this study was to investigate the test–retest reproducibility of k_{ref} values of L-[β-^{11}C]DOPA and that of BP_{ND} of [^{18}F]FE-PE2I in the striatum and midbrain in healthy humans.**

Materials and methods **Twelve healthy male volunteers underwent two PET studies on separate days. Each PET study comprised two PET scans, one with L-[β-^{11}C]DOPA and the other with [^{18}F]FE-PE2I. Volumes of interest were defined for the caudate, putamen, midbrain, and thalamus. Test–retest reproducibility was assessed in terms of intrasubject variability (absolute variability) and reliability [intraclass correlation coefficient (ICC)].**

Results **The absolute variability values of k_{ref} and BP_{ND} were 4.8–25.7% on average for the caudate, putamen, midbrain, and thalamus. The ICC values of the k_{ref} values of L-[β-^{11}C]DOPA were 0.78, 0.71, 0.77, and 0.77 for the caudate, putamen, midbrain, and thalamus, respectively. The ICC values of the BP_{ND} of [^{18}F]FE-PE2I were 0.83, 0.88, 0.71, and 0.70 for the caudate, putamen, midbrain, and thalamus, respectively.**

Conclusion **We found good test–retest reproducibility for the k_{ref} values of L-[β-^{11}C]DOPA and that for the BP_{ND} of [^{18}F]FE-PE2I in the striatum and midbrain, indicating the reliability of clinical investigation using PET with L-[β-^{11}C]DOPA and [^{18}F]FE-PE2I.** *Nucl Med Commun* **35:231–237 © 2014 Wolters Kluwer Health | Lippincott Williams & Wilkins.**

Nuclear Medicine Communications 2014, 35:231–237

Keywords: [^{18}F]FE-PE2I, dopamine synthesis, dopamine transporter, L-[β-^{11}C]DOPA, positron emission tomography

[a]Molecular Neuroimaging Program, [b]Biophysics Program, [c]Molecular Probe Program, Molecular Imaging Center, National Institute of Radiological Sciences, Chiba, [d]Department of Neuropsychiatry, Nippon Medical School, Tokyo, Japan and [e]Department of Clinical Neuroscience, Karolinska Institutet, Psychiatry Section, Stockholm, Sweden

Correspondence to Hiroshi Ito, MD, PhD, Biophysics Program, Molecular Imaging Center, National Institute of Radiological Sciences, 4-9-1 Anagawa, Inage-ku, Chiba-shi, Chiba 263-8555, Japan
Tel: +81 43 206 4702; fax: +81 43 206 0819; e-mail: hito@nirs.go.jp

Received 28 August 2013 **Revised** 30 September 2013
Accepted 21 October 2013

Introduction

Presynaptic dopaminergic function plays a crucial role in the regulation of dopaminergic neurotransmission, and the function includes synthesis and reuptake of endogenous dopamine. Dopamine synthesis capacity can be measured using L-[β-^{11}C]DOPA. L-[β-^{11}C]DOPA is ^{11}C-labelled L-DOPA that can be used as a PET tracer to assess the rate of endogenous dopamine synthesis, which indicates the relative activity of cerebral aromatic L-amino acid decarboxylase [1–3]. Dopamine transporter (DAT) availability can be assessed with [^{18}F]FE-PE2I. Although several radioligands for quantifying DAT availability, such as [^{123}I]-β-CIT and [^{123}I]FP-CIT, have been developed [4,5], [^{18}F]FE-PE2I is characterized by a higher affinity for DAT (k_i: 12 nmol/l) as well as selectivity for DAT relative to serotonin transporter in the striatum (83, [6–8]) compared with conventional radioligands; moreover, the reliable quantification of striatal DAT binding in humans has been shown [9,10].

Recently, alteration of presynaptic dopaminergic function was reported in patients with schizophrenia. Previous PET studies have indicated elevated striatal dopamine synthesis capacity (k_{ref}) in patients with schizophrenia [11,12]. In contrast, a PET study with [^{11}C]PE2I, which has high affinity for DAT in the striatum (k_i: 17 nmol/l), reported elevated DAT availability in the thalamus of patients with schizophrenia [13]. These studies indicated increased dopamine turnover in patients with schizophrenia. Because there is a significant positive correlation between presynaptic dopaminergic function and positive

0143-3636 © 2014 Wolters Kluwer Health | Lippincott Williams & Wilkins

DOI: 10.1097/MNM.0000000000000052

symptoms such as hallucinations and delusions [12], presynaptic dopaminergic function can reflect the severity of positive symptoms. Accordingly, both k_{ref} of L-[β-^{11}C]DOPA and the nondisplaceable binding potential (BP_{ND}) of [^{18}F]FE-PE2I can be elevated and can have a positive correlation in patients with schizophrenia. This indicates that these values and these correlation coefficients can be potential markers for evaluation of the severity of positive symptoms. However, the test–retest reproducibility of k_{ref} values of L-[β-^{11}C]DOPA and that of BP_{ND} of [^{18}F]FE-PE2I and their relationships have not been investigated in healthy individuals, despite one previous study reporting good test–retest reproducibility of k_{ref} values of L-[β-^{11}C]DOPA [14].

The purpose of the present study was to investigate the test–retest reproducibility of the dopamine synthesis capacity by L-[β-^{11}C]DOPA and that of DAT binding by [^{18}F]FE-PE2I in the striatum and midbrain in healthy humans. Test–retest reproducibility was assessed in terms of intrasubject variability (absolute variability) and reliability [intraclass correlation coefficient (ICC)].

Materials and methods

Participants

Twelve healthy male volunteers (age range: 20–39, mean±SD: 24.8±4.7) were recruited and written informed consent was obtained. T1-weighted MRI was normal on visual inspection. None had a history of psychiatric or neurological disorders, and they were free of physical disease. None had substance abuse and/or dependence according to *Diagnostic and Statistical Manual of Mental Disorders*, 4th ed. (DSM-IV) criteria. This study protocol was approved by the Institutional Review Board of the National Institute of Radiological Sciences, Chiba, Japan.

PET procedures

All PET studies were performed with a SET-3000 GCT/X (Shimadzu Corp., Kyoto, Japan) [15], which provides 99 sections with an axial field of view of 26 cm. The intrinsic spatial resolution was 3.4 mm in-plane and 5.0 mm full-width at half-maximum axially. With a Gaussian filter (cutoff frequency: 0.3 cycle/pixel), the reconstructed in-plane resolution was 7.5 mm full-width at half-maximum. Data were acquired in three-dimensional mode. Scatter correction was performed by a hybrid scatter correction method based on acquisition with dual-energy window setting [16]. A 4-min transmission scan using a ^{137}Cs line source was performed for correction of attenuation.

All participants underwent two PET studies on separate days (Scan 1 and Scan 2). Each PET study comprised two PET scans with L-[β-^{11}C]DOPA and [^{18}F]FE-PE2I. The average interval between the two studies was 13.3±17.5 days (mean±SD).

After an intravenous rapid bolus injection of L-[β-^{11}C]DOPA, a dynamic PET scan was taken for 89 min. Ninety minutes after the end of L-[β-^{11}C]DOPA PET measurement, a dynamic PET scan was taken for 90 min after an intravenous rapid bolus injection of [^{18}F]FE-PE2I. The frame sequence consisted of seven 60-s frames, five 120-s frames, four 180-s frames, and 12 300-s frames for L-[β-^{11}C]DOPA, and nine 20-s frames, five 60-s frames, four 120-s frames, 11 240-s frames, and six 300-s frames for [^{18}F]FE-PE2I. The injected radioactivities for L-[β-^{11}C]DOPA and [^{18}F]FE-PE2I in Scan 1 were 199–398 and 167–372 MBq, respectively, and those in Scan 2 were 334–399 and 172–199 MBq, respectively. The specific radioactivities for L-[β-^{11}C]DOPA and [^{18}F]FE-PE2I in Scan 1 were 37–281 and 90–348 GBq/μmol, respectively, and those in Scan 2 were 50–89 and 184–374 GBq/μmol, respectively. Mass doses for L-[β-^{11}C]DOPA and [^{18}F]FE-PE2I in Scan 1 were 5.68±2.80 and 1.00±0.76 nmol, respectively, and those in Scan 2 were 12.44±20.00 and 0.72±0.20 nmol, respectively. No order effects were found in injected radioactivity ($P = 0.50$ and 0.37), specific radioactivity ($P = 0.12$ and 0.95), and mass dose ($P = 0.28$ and 0.27) of L-[β-^{11}C]DOPA and [^{18}F]FE-PE2I by paired t-test.

MRI procedures

All MR images were acquired with a Siemens MAGNETOM Verio 3.0T MR scanner (Siemens AG, Munich, Germany). T1-weighted images were acquired by three-dimensional MPRAGE sequence (TR: 2300 ms; TE: 2.98 ms; flip angle: 9°; field of view: 256 mm; acquisition matrix size: 256 × 256; slice thickness: 1.2 mm).

Graphical analysis

The uptake rate constant for L-[β-^{11}C]DOPA, indicating the dopamine synthesis capacity, was estimated using graphical analysis [17–19], which allows for the calculation of the uptake rate constant (k_{ref}) using time–activity data in a reference brain region with no irreversible binding. k_{ref} values can be estimated by using simple linear least-squares fitting as follows:

$$\frac{C(t)}{C_i'(t)} = k_{ref} \times \frac{\int_0^t C_i'(\tau)d\tau}{C_i'(\tau)} + F \times t > t*,$$

where C_i and C_i' are the total radioactivity concentrations in a brain region with and without irreversible binding, respectively, and t^* is the equilibrium time of the compartment for unchanged radiotracer in brain tissue. Plotting $C_i(t)/C_i'(t)$ versus $\int_0^t C_i'(\tau)d\tau/C_i'(t)$, after time t^*, yields a straight line with the slope k_{ref} and intercept F. In the present study, the occipital cortical region was used as the reference region with no irreversible binding, because this region is known to have the lowest dopamine concentration [20] and lowest L-amino acid decarboxylase activity [21]. The equilibrium time t^* was set to be 29 min, and data plots of 29–89 min were used for linear least-squares fitting [17,22].

Simplified reference tissue model method

DAT availability was quantified using the three-parameter simplified reference tissue model (SRTM) method [23]. The cerebellar cortical region was used as reference tissue because of its negligible availability of DATs. The model allows the estimation of BP_{ND}, which was defined as follows:

$$BP_{ND} = f_{ND} \times B_{avail} / K_D,$$

where f_{ND} is the free fraction of radioligand in the nondisplaceable tissue compartment, B_{avail} indicates the neuroreceptor availability, and K_D indicates the dissociation constant of radioligand to transporters [24]. The SRTM method, assuming that both target and reference regions have the same level of nondisplaceable binding, can be used to describe time–activity curves in the target region as follows [23]:

$$C_T(t) = R_1 \times C_R(t) + \left(k_2 - \frac{R_1 \times k_2}{1+BP_{ND}}\right) \times C_R(t) \otimes \exp\left(-\frac{k_2 \times t}{1+BP_{ND}}\right),$$

where $C_T(t)$ is the total radioactivity concentration in a brain region measured by PET, R_1 is the ratio of K_1 to K_1' (K_1, influx rate constant for the brain target region; K_1', influx rate constant for the reference region), $C_R(t)$ is the radioactivity concentration in the reference region (cerebellum), and $\otimes$ denotes the convolution integral. Parameters R_1, k_2, and BP_{ND} in this model were estimated by the nonlinear curve fitting procedure.

Assessment of test–retest reproducibility

Test–retest reproducibility was assessed in terms of intrasubject variability and test–retest reliability. The absolute variability was defined as the absolute value of the difference between the Scan 1 and Scan 2 measurements expressed as the percentage of the mean value of the two measurements.

$$\text{Var}(\%) = \left|\frac{\text{Scan 1} - \text{Scan 2}}{(\text{Scan 1} + \text{Scan 2}) \times 0.5}\right| \times 100.$$

A measure of the test–retest reliability was assessed by the ICC according to the following equation:

$$\text{ICC} = \frac{\text{MSBS} - \text{MSWS}}{\text{MSBS} + \text{MSWS}},$$

where MSBS is the mean sum of squares between subjects, and MSWS is the mean sum of squares within subjects. This coefficient is an estimate of the reliability of the two sets of measurement and varies from −1 (no reliability) to +1 (perfect reliability – that is, identical test and retest measurements). The ICC value is used as a measure of test–retest reliability. ICC values lower than 0.4 are regarded as poor (low), those between 0.4 and 0.75 are regarded as adequate (middle), and those higher than 0.75 are regarded as excellent (high) test–retest reliability [25].

Assessment of intrasubject variations of L-[β-^{11}C]DOPA and [^{18}F]FE-PE2I

The relationship between intrasubject variations of L-[β-^{11}C]DOPA and [^{18}F]FE-PE2I binding was assessed by Δk_{ref} and ΔBP. Δk_{ref} was defined as the value of the difference between Scan 1 k_{ref} and Scan 2 k_{ref} expressed as the percentage of the mean value of the two k_{ref} values measured with L-[β-^{11}C]DOPA. ΔBP was defined as the value of the difference between Scan 1 BP_{ND} and Scan 2 BP_{ND} expressed as the percentage of the mean value of the two BP_{ND} values measured with [^{18}F]FE-PE2I. Note that Δk_{ref} and ΔBP are not absolute values in comparison with absolute variability (Var).

$$\Delta k_{ref} = \frac{\text{Scan 1} - \text{Scan 2}}{(\text{Scan 1} + \text{Scan 2}) \times 0.5} \times 100.$$

$$\Delta BP = \frac{\text{Scan 1} - \text{Scan 2}}{(\text{Scan 1} + \text{Scan 2}) \times 0.5} \times 100.$$

Data analysis

Calculation of dopamine synthesis capacity and dopamine transporter availability

All data analyses were performed with PMOD 3.2 software (PMOD Technologies, Zurich, Switzerland), Prism 5.0 software (Graphpad Software Inc., San Diego, California, USA), and SPSS (SPSS Inc., Chicago, Illinois, USA) for the evaluation of ICC. Motion corrections were performed frame by frame with normalized mutual information after 6 mm Gaussian filtration for each frame image. Each individual MR image was coregistered to the corresponding summated PET image with normalized mutual information implemented in PMOD 3.2. Volumes of interest (VOIs) were manually drawn on each of the coregistered MR images for the caudate, putamen, midbrain, thalamus, occipital, and cerebellar cortical regions according to a previous report [26] (Fig. 1). The reference region of L-[β-^{11}C]DOPA was defined for the occipital cortical region and that of [^{18}F]FE-PE2I was defined for the cerebellar cortical region. The mean size of each VOI across 12 participants was $1.53 \pm 0.63\,cm^3$ for the caudate, $3.28 \pm 0.73\,cm^3$ for the putamen, $0.78 \pm 0.23\,cm^3$ for the midbrain, $3.79 \pm 0.89\,cm^3$ for the thalamus, $4.79 \pm 0.45\,cm^3$ for the occipital cortical region, and $9.74 \pm 1.42\,cm^3$ for the cerebellar cortical region (mean ± SD). Subsequently, to obtain regional time–activity curves, regional radioactivity was calculated for each frame, corrected for decay, and plotted versus time. Consequently, for the caudate, putamen, midbrain, and thalamus, k_{ref} of L-[β-^{11}C]DOPA, the dopamine uptake rate constant, was calculated with a Gjedde–Patlak plot. BP_{ND} of [^{18}F]FE-PE2I, reflecting DAT availability, was calculated using the SRTM method.

Assessment of test–retest reproducibility

All statistical data are shown as mean ± SD. Subsequently, to evaluate test–retest reproducibility of each radioligand, absolute variability and ICC values of k_{ref} of

Fig. 1

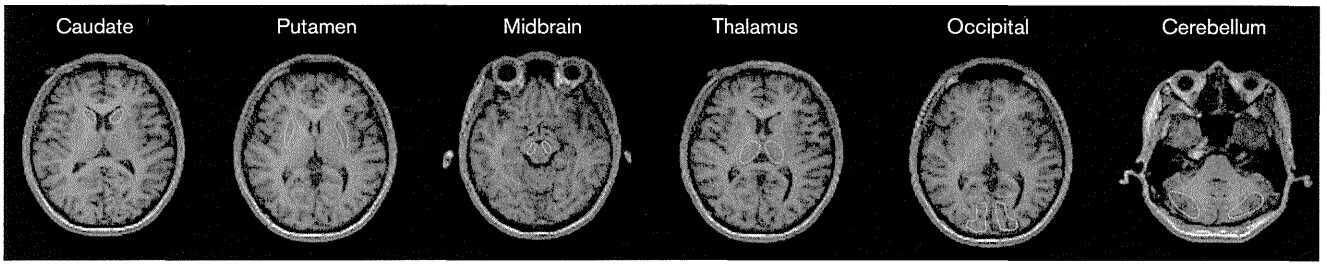

Volumes of interest (VOIs) in a representative individual. VOIs were drawn manually on each of the coregistered MR images for the caudate, putamen, midbrain, thalamus, occipital, and cerebellar cortical.

L-[β-^{11}C]DOPA and those of BP_{ND} of [^{18}F]FE-PE2I were calculated.

Results

Test–retest reproducibility of dopamine uptake rate constant of L-[β-^{11}C]DOPA

Table 1 shows the test–retest reproducibility of the k_{ref} value estimated by L-[β-^{11}C]DOPA. The absolute variability of the k_{ref} values was 10.7±5.4, 11.9±5.8, 13.1±10.5, and 25.7±26.6 (mean±SD) for the caudate, putamen, midbrain, and thalamus, respectively. The ICC values of the k_{ref} values of L-[β-^{11}C]DOPA were 0.78, 0.71, 0.77, and 0.77 in the caudate, putamen, midbrain and thalamus, respectively.

Test–retest reproducibility of the dopamine transporter binding potential of [^{18}F]FE-PE2I

Table 1 shows the test–retest reproducibility of the BP_{ND} value estimated by [^{18}F]FE-PE2I. The absolute variability of BP_{ND} of [^{18}F]FE-PE2I was 4.8±5.3, 5.6±2.7, 9.7±8.2, and 15.8±11.9 (mean±SD) for the caudate, putamen, midbrain, and thalamus, respectively. The ICC values of BP_{ND} of [^{18}F]FE-PE2I were 0.83, 0.88, 0.71, and 0.70 in the caudate, putamen, midbrain, and thalamus, respectively.

Relationship between intrasubject variations of L-[β-^{11}C]DOPA and [^{18}F]FE-PE2I binding

Figure 2 shows the correlation analysis of intrasubject variability between L-[β-^{11}C]DOPA and [^{18}F]FE-PE2I (Δk_{ref} and ΔBP_{ND}) in the caudate and putamen. No significant correlation was observed in the caudate and putamen ($r = -0.14$, $P = 0.67$, for the caudate and $r = -0.45$, $P = 0.14$, for the putamen).

Discussion

In the present study, we found good test–retest reproducibility of the k_{ref} values of L-[β-^{11}C]DOPA and that of the BP_{ND} of [^{18}F]FE-PE2I in the caudate, putamen, midbrain, and thalamus.

Table 1 Regional k_{ref} values from L-[β-^{11}C]DOPA for Scan 1 and Scan 2, and their test–retest reproducibility from the Gjedde–Patlak method in individual PET space; and regional BP_{ND} values from [^{18}F]FE-PE2I for Scan 1 and Scan 2, and their test–retest reproducibility from the simplified reference tissue model method in individual PET space

	Mean±SD			
Region	Scan 1 COV (%)	Scan 2 COV (%)	Var (%)	ICC
Caudate				
L-[β-^{11}C]DOPA	0.0094±0.0016 16.7	0.0098±0.0021 21.4	10.7±5.4	0.78
[^{18}F]FE-PE2I	3.18±0.36 11.4	3.25±0.29 9.1	4.8±5.3	0.83
Putamen				
L-[β-^{11}C]DOPA	0.0112±0.0019 16.6	0.0116±0.0020 17.6	11.9±5.8	0.71
[^{18}F]FE-PE2I	3.30±0.38 11.5	3.42±0.44 12.7	5.6±2.7	0.88
Midbrain				
L-[β-^{11}C]DOPA	0.0065±0.0015 22.8	0.0061±0.0014 23.1	13.1±10.5	0.77
[^{18}F]FE-PE2I	0.61±0.11 17.9	0.64±0.10 15.2	9.7±8.2	0.71
Thalamus				
L-[β-^{11}C]DOPA	0.0022±0.0010 45.4	0.0020±0.0011 54.0	25.7±26.6	0.77
[^{18}F]FE-PE2I	0.33±0.08 25.1	0.35±0.12 33.6	15.8±11.9	0.70

COV, change of variation; ICC, intraclass correlation coefficient; Var, absolute variability.

Test–retest reproducibility of the dopamine uptake rate constant of L-[β-^{11}C]DOPA

L-[β-^{11}C]DOPA showed good test–retest reproducibility in the caudate, putamen, midbrain, and thalamus. The present study replicated previous test–retest reproducibility PET studies using L-[β-^{11}C]DOPA and 6-[^{18}F]-L-DOPA [14,27]. As for the test–retest reproducibility of the k_{ref} values of L-[β-^{11}C]DOPA, Ota *et al.* [14] reported 7.3±6.5, 7.3±2.4, and 9.2±9.6% intrasubject variability values and 0.73, 0.51, and 0.71 ICC values for the caudate, putamen, and midbrain, respectively. As for the test–retest reproducibility of 6-[^{18}F]-L-DOPA, Vingerhoets *et al.* [27] reported 10.3 and 8.9% intrasubject variability values and 0.82 and 0.85 ICC values for the caudate and putamen, respectively. These results were

Fig. 2

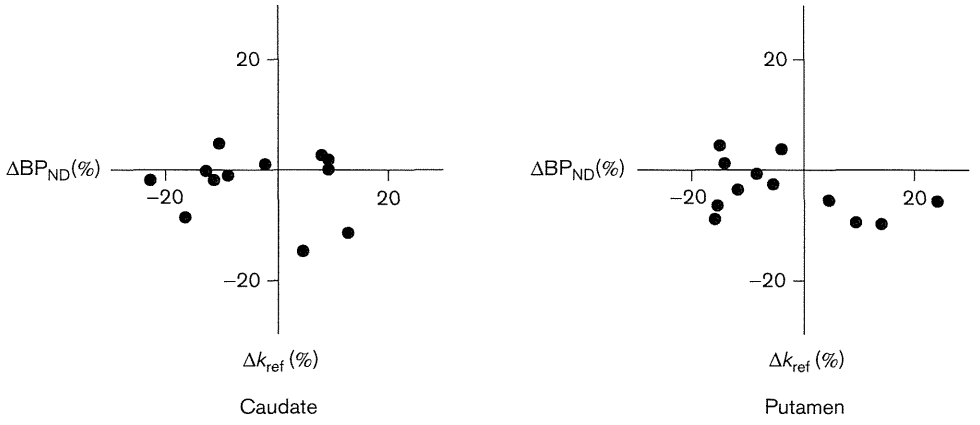

Relationship of intrasubject variations between L-[β-^{11}C]DOPA and [^{18}F]FE-PE2I (Δk_{ref} and ΔBP$_{ND}$) in the caudate and putamen. Correlation analysis showed no significant relationship in the caudate and putamen.

similar to the present results (Table 1), indicating good test–retest reproducibility for the k_{ref} values of L-[β-^{11}C]DOPA in these regions. In the putamen, the estimated intergroup difference of mean k_{ref} values under 0.05 of α and 0.2 of β in 12 participants was 0.0024 under 0.002 of SD, indicating that a difference of 21% from the control k_{ref} value can be examined by the paired t-test (estimated from the mean and SD of the putaminal k_{ref} value of Scan 2).

The intrasubject variability of the k_{ref} values of L-[β-^{11}C]DOPA was larger than that of BP$_{ND}$ of [^{18}F]FE-PE2I. The difference in the intrasubject variability could be derived from the difference in signal-to-noise ratios (SNRs) of brain uptake between L-[β-^{11}C]DOPA and [^{18}F]FE-PE2I. Ito *et al.* [22] reported that the ratio of specific binding (putamen) to nonspecific binding (occipital cortex) of L-[β-^{11}C]DOPA (29–89 min), reflecting SNRs, was 2.46, whereas Sasaki *et al.* [9] reported that the ratio was 6.0. This three-fold difference in SNRs can cause the large intrasubject variability in the k_{ref} values of L-[β-^{11}C]DOPA.

Test–retest reproducibility of the binding potential of [^{18}F]FE-PE2I

[^{18}F]FE-PE2I showed good test–retest reproducibility in the caudate, putamen, midbrain, and thalamus. The present study replicated a previous test–retest reproducibility PET study on [^{11}C]PE2I [28]. As for the test–retest reproducibility of [^{11}C]PE2I, Hirvonen *et al.* [28] reported 8.9±4.2, 4.8±6.2, and 6.5±5.2% intrasubject variability values and 0.48, 0.48, and 0.83 ICC values for the caudate, putamen, and midbrain, respectively. These results were similar to the present results (Table 1), indicating good test–retest reproducibility for the BP$_{ND}$ of [^{18}F]FE-PE2I in these regions. In the putamen, the estimated intergroup difference of mean BP$_{ND}$ values under 0.05 of α and 0.2 of β in 12 participants was 0.53 under 0.44 of SD, indicating that a difference of 15% from the control BP$_{ND}$ value can be examined by means of the paired t-test (estimated from mean and SD of the putaminal BP$_{ND}$ value of Scan 2).

[^{18}F]FE-PE2I showed similar test–retest reproducibility compared with conventional radioligands such as [^{123}I]β-CIT and [^{123}I]FP-CIT. Seibyl *et al.* [29] reported 6.6±4.3% intrasubject variability values and 0.98 ICC values for [^{123}I]β-CIT in the striatum. Similarly, Tsuchida *et al.* [30] reported 5.5±4.1% intrasubject variability values and 0.89 ICC values for [^{123}I]FP-CIT in the striatum. Moreover, [^{18}F]FE-PE2I has higher selectivity for DAT relative to serotonin transporter compared with [^{123}I]β-CIT and [^{123}I]FP-CIT, indicating that [^{18}F]FE-PE2I can selectively measure DAT availability with low intrasubject and intersubject variability.

Relationship between the intrasubject variations of dopamine uptake rate constant of L-[β-^{11}C]DOPA and that of the binding potential of [^{18}F]FE-PE2I

We found no significant correlation between the intrasubject variations of the k_{ref} values of L-[β-^{11}C]DOPA and that of BP$_{ND}$ of [^{18}F]FE-PE2I in the caudate and putamen. These intrasubject variations can include both random noise and physiological change of presynaptic dopaminergic function between the two measurements. Although the observed intrasubject variations for each radioligand can include both components, as for the relationship between k_{ref} and BP$_{ND}$ values, it mostly includes random noise and not the physiological correspondence between dopamine synthesis and DAT availability. Therefore, this result indicates that there is little physiological relationship of intrasubject variations between k_{ref} of L-[β-^{11}C]DOPA and BP$_{ND}$ of [^{18}F]FE-PE2I in healthy individuals. Although the present study indicates that, in healthy individuals, there

was negligible relationship between intrasubject variability in k_{ref} values and that of BP_{ND} at resting state, little has been investigated as to whether such findings are replicated at conditions in which dopaminergic neurotransmission increases. To reinforce our results, further studies would be needed, such as to determine whether these intrasubject variabilities are related to motor tasks that enhance dopaminergic neurotransmission.

In addition, in this study, we found no significant correlation between k_{ref} values of L-[β-^{11}C]DOPA and BP_{ND} of [^{18}F]FE-PE2I in the caudate and putamen in healthy individuals (data not shown). In contrast, in patients with schizophrenia, both dopamine synthesis capacity [11,12] and DAT availability [13] are reported to be elevated. This indicates that, in schizophrenia, there can be a dynamic relationship between dopamine synthesis and uptake. Whereas pathologically increased dopamine release provides a link between dopamine synthesis and uptake, normal dopamine release might not.

Our PET paradigm can be useful for investigating the pathophysiology of the longitudinal alteration of the presynaptic dopaminergic function of Parkinson's disease (PD). In the course of progression, dopamine synthesis capacity and DAT availability are expected to decrease exponentially in patients with PD [31,32]. However, with regard to dopamine synthesis capacity in PD in early stage, several arguments have been put forward. Although some reports suggest that dopamine synthesis capacity is elevated in patients with PD in early stage [33], a decrease has also been reported [34]. Such various alteration patterns in early stage might be explained by the complementary compensation between dopamine synthesis and uptake. Further studies on the intrasubject variation between dopamine synthesis capacity and DAT availability could help elucidate such various processes.

Limitations

We should acknowledge some limitations in the present study. Even though we carefully referred to previous reports on the analytic procedure and control for the size of VOI, subtle registration errors might have occurred when VOIs were manually drawn on coregistered MR images. Further studies would be needed for a better registration process. As for correlation analysis between intrasubject variations of k_{ref} and BP_{ND}, our post-hoc analysis indicates that the present study had a rather smaller sample size than expected (398 for caudate and 36 for putamen). Therefore, we could not conclude that there is no physiological relationship between dopamine synthesis capacity and DAT availability.

Conclusion

We found a good test–retest reproducibility of k_{ref} values of L-[β-^{11}C]DOPA and that of BP_{ND} of [^{18}F]FE-PE2I in the caudate, putamen, midbrain, and thalamus. The results of the present study confirmed the reliability of measurements taken with L-[β-^{11}C]DOPA and [^{18}F]FE-PE2I.

Acknowledgements

The authors thank Katsuyuki Tanimoto and Takahiro Shiraishi for their assistance in performing the PET experiments and Izumi Izumida and Kazuko Suzuki for their help as clinical research coordinators at the National Institute of Radiological Sciences.

A part of this study is the result of 'Integrated research on neuropsychiatric disorders' carried out under the Strategic Research Program for Brain Sciences by the Ministry of Education, Culture, Sports, Science and Technology of Japan.

Conflicts of interest

There are no conflicts of interest.

References

1 Korf J, Reiffers S, Beerling-Van Der Molen H, Lakke J, Paans A, Vaalburg W, *et al.* Rapid decarboxylation of carbon-11 labelled DL-DOPA in the brain: a potential approach for external detection of nervous structures. *Brain Res* 1978; **145**:59–67.

2 Tedroff J, Aquilonius SM, Hartvig P, Lundqvist H, Bjurling P, Långström B. Estimation of regional cerebral utilization of [^{11}C]-L-3, 4-dihydroxyphenylalanine (DOPA) in the primate by positron emission tomography. *Acta Neurol Scand* 1992; **85**:166–173.

3 Hartvig P, Ågren H, Reibring L, Tedroff J, Bjurling P, Kihlberg T, *et al.* Brain kinetics of L-[β-^{11}C]dopa in humans studied by positron emission tomography. *J Neural Transm* 1991; **86**:25–41.

4 Brücke T, Kornhuber J, Angelberger P, Asenbaum S, Frassine H, Podreka I. SPECT imaging of dopamine and serotonin transporters with [^{123}I]β-CIT. Binding kinetics in the human brain. *J Neural Transm* 1993; **94**:137–146.

5 Kuikka JT, Bergström KA, Ahonen A, Hiltunen J, Haukka J, Länsimiese E, *et al.* Comparison of iodine-123 labelled 2β-carbomethoxy-3β-(4-iodophenyl) tropane and 2β-carbomethoxy-3β-(4-iodophenyl)-N-(3-fluoropropyl) nortropane for imaging of the dopamine transporter in the living human brain. *Eur J Nucl Med* 1995; **22**:356–360.

6 Varrone A, Steiger C, Schou M, Takano A, Finnema SJ, Guilloteau D, *et al.* In vitro autoradiography and in vivo evaluation in cynomolgus monkey of [^{18}F]FE-PE2I, a new dopamine transporter PET radioligand. *Synapse* 2009; **63**:871–880.

7 Schou M, Steiger C, Varrone A, Guilloteau D, Halldin C. Synthesis, radiolabeling and preliminary in vivo evaluation of [^{18}F]FE-PE2I, a new probe for the dopamine transporter. *Bioorg Med Chem Lett* 2009; **19**:4843–4845.

8 Stepanov V, Schou M, Jarv J, Halldin C. Synthesis of ^{3}H-labeled N-(3-iodoprop-2E-enyl)-2beta-carbomethoxy-3beta-(4-methylphenyl)nortropane (PE2I) and its interaction with mice striatal membrane fragments. *Appl Radiat Isot* 2007; **65**:293–300.

9 Sasaki T, Ito H, Kimura Y, Arakawa R, Takano H, Seki C, *et al.* Quantification of dopamine transporter in human brain using PET with ^{18}F-FE-PE2I. *J Nucl Med* 2012; **53**:1065–1073.

10 Varrone A, Tóth M, Steiger C, Takano A, Guilloteau D, Ichise M, *et al.* Kinetic analysis and quantification of the dopamine transporter in the nonhuman primate brain with ^{11}C-PE2I and ^{18}F-FE-PE2I. *J Nucl Med* 2011; **52**:132–139.

11 Fusar-Poli P, Meyer-Lindenberg A. Striatal presynaptic dopamine in schizophrenia, Part II: meta-analysis of [^{18}F/^{11}C]-DOPA PET studies. *Schizophr Bull* 2013; **39**:33–42.

12 Nozaki S, Kato M, Takano H, Ito H, Takahashi H, Arakawa R, *et al.* Regional dopamine synthesis in patients with schizophrenia using L-[β-^{11}C]DOPA PET. *Schizophr Res* 2009; **108**:78–84.

13 Arakawa R, Ichimiya T, Ito H, Takano A, Okumura M, Takahashi H, *et al.* Increase in thalamic binding of [^{11}C]PE2I in patients with schizophrenia:

a positron emission tomography study of dopamine transporter. *J Psychiatr Res* 2009; **43**:1219–1223.
14 Ota M, Yasuno F, Ito H, Seki C, Nozaki S, Asada T, *et al.* Age-related decline of dopamine synthesis in the living human brain measured by positron emission tomography with L-[β-^{11}C]DOPA. *Life Sci* 2006; **79**:730–736.
15 Matsumoto K, Kitamura K, Mizuta T, Tanaka K, Yamamoto S, Sakamoto S, *et al.* Performance characteristics of a new 3-dimensional continuous-emission and spiral-transmission high-sensitivity and high-resolution PET camera evaluated with the NEMA NU 2-2001 standard. *J Nucl Med* 2006; **47**:83–90.
16 Ishikawa A, Kitamura K, Mizuta T, Tanaka K, Amano M, Inoue Y, *et al.* Implementation of on-the-fly scatter correction using dual energy window method in continuous 3D whole body PET scanning. *Nucl Sci Symp Conf Rec* 2005; **5**:2497–2500.
17 Ito H, Ota M, Ikoma Y, Seki C, Yasuno F, Takano A, *et al.* Quantitative analysis of dopamine synthesis in human brain using positron emission tomography with L-[β-^{11}C]DOPA. *Nucl Med Commun* 2006; **27**:723–731.
18 Gjedde A. *Exchange diffusion of large neutral amino acids between blood and brain.* New York: Stockton Press; 1988.
19 Patlak CS, Blasberg RG. Graphical evaluation of blood-to-brain transfer constants from multiple-time uptake data. Generalizations. *J Cereb Blood Flow Metab* 1985; **5**:584–590.
20 Brown RM, Crane AM, Goldman PS. Regional distribution of monoamines in the cerebral cortex and subcortical structures of the rhesus monkey: concentrations and in vivo synthesis rates. *Brain Res* 1979; **168**:133–150.
21 Lloyd K, Hornykiewicz O. Occurrence and distribution of aromatic L-amino acid (L-DOPA) decarboxylase in the human brain. *J Neurochem* 1972; **19**:1549–1559.
22 Ito H, Shidahara M, Takano H, Takahashi H, Nozaki S, Suhara T. Mapping of central dopamine synthesis in man, using positron emission tomography with L-[β-^{11}C]DOPA. *Ann Nucl Med* 2007; **21**:355–360.
23 Lammertsma AA, Hume SP. Simplified reference tissue model for PET receptor studies. *Neuroimage* 1996; **4**:153–158.
24 Innis RB, Cunningham VJ, Delforge J, Fujita M, Gjedde A, Gunn RN, *et al.* Consensus nomenclature for in vivo imaging of reversibly binding radioligands. *J Cereb Blood Flow Metab* 2007; **27**:1533–1539.
25 Fleiss JL. *The design and analysis of clinical experiments.* New York: Wiley; 1986.
26 Ito H, Takahashi H, Arakawa R, Takano H, Suhara T. Normal database of dopaminergic neurotransmission system in human brain measured by positron emission tomography. *Neuroimage* 2008; **39**:555–565.
27 Vingerhoets FJ, Snow BJ, Schulzer M, Morrison S, Ruth TJ, Holden JE, *et al.* Reproducibility of fluorine-18-6-fluorodopa positron emission tomography in normal human subjects. *J Nucl Med* 1994; **35**:18–24.
28 Hirvonen J, Johansson J, Teras M, Oikonen V, Lumme V, Virsu P, *et al.* Measurement of striatal and extrastriatal dopamine transporter binding with high-resolution PET and [^{11}C]PE2I: quantitative modeling and test–retest reproducibility. *J Cereb Blood Flow Metab* 2008; **28**:1059–1069.
29 Seibyl JP, Laruelle M, van Dyck CH, Wallace E, Baldwin RM, Zoghbi S, *et al.* Reproducibility of iodine-123-β-CIT SPECT brain measurement of dopamine transporters. *J Nucl Med* 1996; **37**:222–228.
30 Tsuchida T, Ballinger JR, Vines D, Kim YJ, Utsunomiya K, Lang AE, *et al.* Reproducibility of dopamine transporter density measured with ^{123}I-FPCIT SPECT in normal control and Parkinson's disease patients. *Ann Nucl Med* 2004; **18**:609–616.
31 Morrish P, Sawle G, Brooks D. An [^{18}F]dopa–PET and clinical study of the rate of progression in Parkinson's disease. *Brain* 1996; **119**:585–591.
32 Pirker W, Djamshidian S, Asenbaum S, Gerschlager W, Tribl G, Hoffmann M, *et al.* Progression of dopaminergic degeneration in Parkinson's disease and atypical parkinsonism: a longitudinal β-CIT SPECT study. *Mov Disord* 2002; **17**:45–53.
33 Lee CS, Samii A, Sossi V, Ruth TJ, Schulzer M, Holden JE, *et al.* In vivo positron emission tomographic evidence for compensatory changes in presynaptic dopaminergic nerve terminals in Parkinson's disease. *Ann Neurol* 2000; **47**:493–503.
34 Eshuis S, Jager P, Maguire R, Jonkman S, Dierckx R, Leenders K. Direct comparison of FP-CIT SPECT and F-DOPA PET in patients with Parkinson's disease and healthy controls. *Eur J Nucl Med* 2009; **36**:454–462.

Psychopharmacology (2014) 231:2321–2325
DOI 10.1007/s00213-013-3392-2

ORIGINAL INVESTIGATION

Effect of mazindol on extracellular dopamine concentration in human brain measured by PET

Takeshi Sakayori · Amane Tateno · Ryosuke Arakawa · Yumiko Ikeda · Hidenori Suzuki · Yoshiro Okubo

Received: 4 August 2013 / Accepted: 28 November 2013 / Published online: 8 January 2014

Abstract
Rationale Mazindol, an appetite suppressant, inhibits the reuptake of dopamine in the synaptic cleft. It has been considered that mazindol might enhance dopamine transmission in the human brain. However, there has been no study that investigated the extracellular dopamine concentration in vivo.
Objective Using positron emission tomography (PET), we aimed to measure the effect of mazindol on the extracellular dopamine concentration and to evaluate how mazindol affects the dopamine system in the healthy human brain.
Methods Eleven healthy individuals (six males, five females, age 30.9 ± 4.9 years) were enrolled in this study. Each participant was scanned with [^{11}C]raclopride on 1 day without any medicine as baseline condition, and on another day with mazindol as drug condition. In the drug condition, participants took mazindol 0.5 mg ($N = 5$) or 1.5 mg ($N = 6$) 2 h before the PET scan. Plasma concentrations of mazindol were measured before the injection of [^{11}C]raclopride, and urine concentrations of mazindol were measured after the scan.
Results After taking mazindol, the calculated decrease in binding potential (ΔBP) in the striatum was 1.74 % for 0.5 mg and 8.14 for 1.5 mg, and the correlation with the blood concentration of mazindol was significant ($P = 0.0016$, $R^2 = 0.69$). ΔBP was not significantly correlated with the urine concentration of mazindol ($P = 0.84$, $R^2 = 0.005$).
Conclusions Mazindol increased the extracellular concentration of dopamine in the human brain, and its effect was dose dependent. A single administration of mazindol, even at usual dosage, elevated dopamine concentration similarly to other addictive drugs, suggesting that the risk of dependence may increase with the mazindol dose.

Keywords Mazindol · Positron emission tomography · [^{11}C]raclopride · Dopamine · Dependence

Background

Mazindol, an appetite suppressant, ameliorates obesity by improving metabolic changes in human, since it enhances heat production, glucose utilization, and energy control (e.g., suppression of feeding and digestion absorption) in its pharmacological action (Minami et al. 1985; Sikdar et al. 1985). Mazindol inhibits the reuptake of noradrenaline and dopamine in nerve endings (Engstrom et al. 1975), and it has been discussed that mazindol might have awakening effect, euphoric effect, and might provoke dependence, since mazindol belongs to amphetamine derivatives in terms of chemical structure (Carruba et al. 1977). There has also been a case report of a patient with obesity presenting with psychiatric symptoms such as irritability, mood enhancement, hyperactivity, and talkativeness after continually taking a prescription dose of mazindol for 5 months (Ito et al. 1995). Mazindol increased locomotor hyperactivity and stereotypic behavior in rats (Nakajima et al. 1986), and the frequency of intake was observed to increase in an intravenous drug self-ingestion test in monkeys (Yanagida et al. 1982), leading to the suggestion of its risks of dependence and abuse. On the other hand, another study reported that there was no dependence of

T. Sakayori · A. Tateno · R. Arakawa · Y. Okubo (✉)
Department of Neuropsychiatry, Graduate School of Medicine, Nippon Medical School, 1-1-5, Sendagi, Bunkyo-ku, Tokyo 113-8602, Japan
e-mail: okubo-y@nms.ac.jp

R. Arakawa
Department of Adult Mental Health, National Institute of Mental Health, National Center of Neurology and Psychiatry, 4-4-1, Ogawahigashicho, Kodaira-city, Tokyo 187-8557, Japan

Y. Ikeda · H. Suzuki
Department of Pharmacology, Graduate School of Medicine, Nippon Medical School, 1-1-5, Sendagi, Bunkyo-ku, Tokyo 113-8602, Japan

mazindol, since mazindol has the isoindole skeleton, which has no effect of promoting noradrenaline and dopamine release, instead of the phenethylamine skeleton of cocaine and amphetamine (Kurihara et al. 1985).

Positron emission tomography (PET) makes it possible to assess monoamine neurotransmitters in vivo. Further, PET and [^{11}C]raclopride can be used to measure changes in extracellular dopamine in the human brain. [^{11}C] raclopride is a ligand that specifically binds to dopamine D_2 receptors in the striatum(Farde et al. 1986). The administration of a psychostimulant is associated with an increase in endogenous dopamine at the synaptic cleft and a reduction in the binding of [^{11}C]raclopride. Thus, the comparison of pre- and post-psychostimulant scans provides a measure of in vivo dopamine release (Laruelle 2000; Carboni et al. 1989). The behavioral effects and the reinforcing properties of amphetamine and cocaine have been suggested to be related to an increase in extracellular dopamine concentration in mesostriatal and mesolimbic areas of the brain (Carboni et al. 1989).

Sufficient information on the action of mazindol in the human brain is necessary for its safe use, but the effect of mazindol on extracellular dopamine concentration is not clear. In this study, we used PET and [^{11}C]raclopride to measure the effect of mazindol on extracellular dopamine concentration.

Methods

Subjects and study design

Eleven healthy individuals (six male, five female, age 30.9± 4.9 years) participated in this study. Inclusion criteria were as follows: (1) nonsmoking, (2) ability to understand and give informed consent, and (3) age of 20–65 years. Exclusion criteria were as follows: (1) current or past history of mental illness or severe physical condition, (2) unable to undergo magnetic resonance imaging (MRI) exam, (3) pregnant or potential pregnancy, (4) allergy to mazindol or caffeine, (5) exposure to more than 15 mSv of radiation a year, and (6) undergoing X-ray examination within 2 days before the PET scan. They had never used mazindol and recreational drugs. Thus, they had no experience with the drug before entering the study. All participants were instructed not to consume caffeine-containing beverages from 2 days before the PET scans, as the dopamine system may be affected by caffeine.

Each participant was scanned with [^{11}C]raclopride on 1 day without any medicine as baseline condition, and on a later day with mazindol as drug condition. They were scanned as baseline condition first, and then as drug condition 1 or 2 weeks later.

For the drug condition, participants took mazindol at 0.5 mg (N=5; initial dose per day in Japan) or 1.5 mg (N= 6; maximum dose per day in Japan) 2 h before the PET scan (i.e., time of maximum plasma concentration of mazindol). Plasma concentrations of mazindol were measured prior to [^{11}C]raclopride injection, and urine concentrations of mazindol were measured after the second PET scans.

The study was approved by the Ethics Committee of the Institutional Review Board of Nippon Medical School, and after complete explanation of the study, written informed consent was obtained from all participants.

Imaging data

A PET scanner system, Eminence SET-3000GCT/X (Shimadzu Corp., Kyoto, Japan), was used to measure regional brain radioactivity. Full width at half maximum (FWHM) was 3.72 mm in body axis and 3.45 mm in cross section. Each scan was preceded by a 4-minute transmission scan for attenuation correction using ^{137}Cs. Dynamic PET scanning was performed for 60 min after intravenous bolus injection of [^{11}C]raclopride. Injected radioactivity was 212.0–236.3 (226.0±1.0; mean±SD) MBq at baseline condition and 214.1–247.2 (231.9±1.0) MBq at drug condition. Specific radioactivity was 58.1–162.2 (93.1±32.8) GBq/μmol at baseline condition and 52.3–104.5 (75.8±16.2) GBq/μmol at drug condition. Injected mass was 0.58–1.49 (1.1±0.3) μg at baseline condition and 0.89–1.55 (1.3±0.3) μg at drug condition. MR images of the brain were acquired with 1.5-T MR imaging, Intera 1.5 T Achieve Nova (Philips Medical Systems, Best, Netherlands). T_1-weighted MR images were obtained at 1-mm slices.

Data analysis

Regions of interest (ROIs) were defined for the striatum (caudate and putamen) and cerebellar cortex. ROIs were drawn manually on summated PET images with reference to coregistered individual MR images. The average values of right and left ROIs were used for the analysis. Dopamine D_2 receptor binding was quantified using a three-parameter simplified reference tissue model (Ito et al. 2001; Lammertsma and Hume 1996). The cerebellum was used as reference region because of its negligible dopamine D_2 receptor density (Suhara et al. 1999). This model allows estimation of the binding potential (BP_{ND}), which was defined as $f_{ND} \times B_{max}/K_d$, where f_{ND} is the free fraction of ligand in the nondisplaceable tissue compartment, B_{max} is the receptor density, and K_d is the dissociation constant (Innis et al. 2007). Based on a previous study (Takahashi et al. 2008), the release of dopamine could be evaluated by calculating the change of BP_{ND} (ΔBP) following mazindol intake. ΔBP was estimated by the following equation:

$\Delta BP=(BP_{baseline}-BP_{drug})/BP_{baseline} \times 100$, where $BP_{baseline}$ is BP_{ND} in the baseline condition, and BP_{drug} is BP_{ND} in the drug condition. Correlation between plasma or urine mazindol

Table 1 Subject characteristics, dose, concentration, BP, and ΔBP

No	age	gender	dose of Maz (mg)	plasma Maz (nM)	plasma M1 (nM)	Urine Maz (Nm)	Urine m1 (nM)	BP base			BP drug			ΔBP (%)		
								striatum	caudate	putamen	striatum	caudate	putamen	striatum	caudate	putamen
1	27	M	0.5	3.57	1.04	254.52	52.33	3.65	2.92	3.91	3.52	3.01	3.71	3.56	-3.08	5.12
2	38	F	0.5	3.93	0.93	49.20	19.67	3.14	2.80	3.27	3.13	2.78	3.27	0.32	0.71	0.00
3	38	F	0.5	3.02	0.73	25.04	14.20	3.37	3.19	3.43	3.37	3.02	3.49	0.00	5.33	-1.75
4	37	M	0.5	2.01	0.00	24.34	8.13	3.77	3.24	1.00	3.65	3.14	3.87	3.18	3.09	3.25
5	27	M	0.5	2.11	1.04	3.07	16.29	3.63	3.10	3.90	3.57	3.17	3.74	1.65	-2.23	4.10
6	28	M	1.5	2.24	1.57	4.95	29.44	3.84	3.32	4.02	3.62	3.17	3.76	5.73	4.52	6.47
7	31	M	1.5	14.04	5.65	49.85	25.14	3.12	2.91	3.22	2.70	2.40	2.85	13.46	17.53	11.49
8	28	F	1.5	8.61	3.52	31.50	19.62	3.73	3.20	3.90	3.51	2.99	3.66	5.90	6.56	6.15
9	33	M	1.5	10.91	4.09	188.6	64.28	3.94	3.26	4.16	3.70	3.08	3.89	6.09	5.52	6.49
10	29	F	1.5	14.45	5.77	10.03	27.33	4.40	3.76	4.57	4.07	3.62	4.20	7.50	3.72	8.10
11	24	F	1.5	13.95	4.13	0.00	26.73	4.04	3.60	4.19	3.63	3.27	3.76	10.15	9.17	10.26

Maz mazindol, *BP* binding potential

levels and ΔBP by mazindol was tested by Pearson's correlation coefficient. A P value of <0.05 was considered statistically significant. The Bonferroni correction was used for multiple comparisons.

Results

Results of our study are shown in Table 1. Five participants (age range 27–38 years) took 0.5 mg and six participants (age range 24–33 years) took 1.5 mg. After mazindol intake, mazindol plasma concentration was 2.93±0.86 nM (mean± SD) (range 2.01–3.93) for 0.5 mg and 10.70±4.73 nM (range 2.24–14.45) for 1.5 mg. Urine concentration was 88.275± 103.75 nM (range 3.07–254.52) for 0.5 mg and 47.49± 71.61 nM (range 0–188.6) for 1.5 mg. Further, urine concentration of mazindol metabolite (M1) was 22.12±17.40 nM (range 8.13–52.33) for 0.5 mg and 32.09±16.11 nM (range 19.62–64.28) for 1.5 mg.

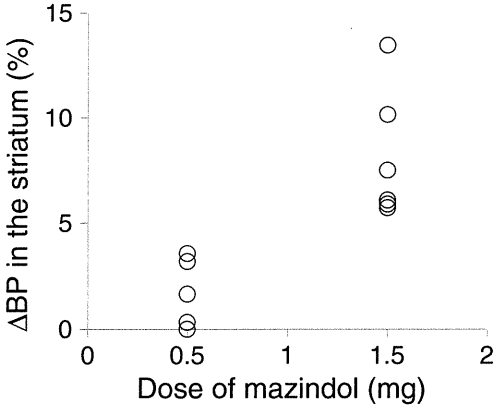

Fig. 1 Scatter plot of ΔBP in the striatum by dose of mazindol

BP_{ND} in the striatum was decreased by 1.74±1.62 % (range 0.00–3.56) for 0.5 mg and 8.14±3.09 % (range 5.73–13.46) for 1.5 mg (Fig. 1). BP_{ND} in the caudate was decreased by 0.76±0.58 % (range −3.08–5.33) for 0.5 mg and 7.84± 3.29 % (range 3.72–9.17) for 1.5 mg. BP_{ND} in the putamen

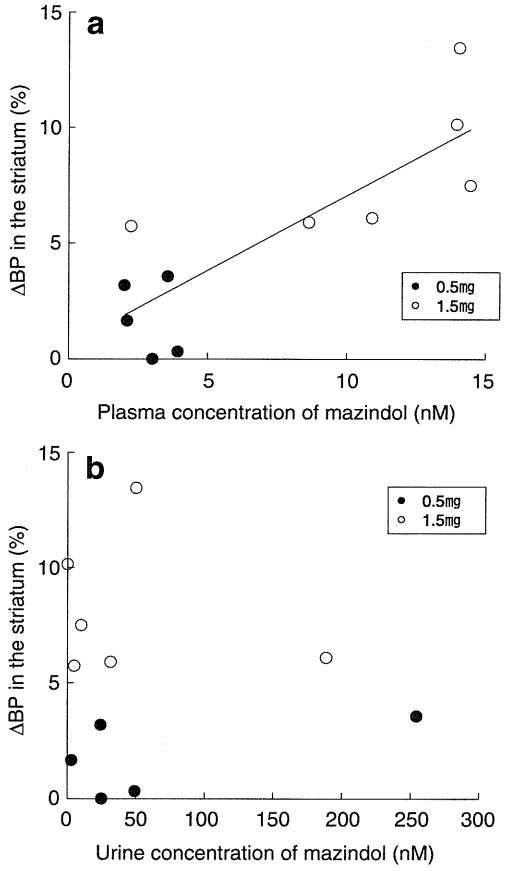

Fig. 2 Relationship between plasma (**a**) or urine (**b**) concentration of mazindol and ΔBP in the striatum

was decreased by 2.14±0.72 % (range −1.75–5.12) for 0.5 mg and 8.16±2.68 % (range 6.47–11.5) for 1.5 mg.

ΔBP in the striatum was significantly correlated with mazindol plasma concentration ($P=0.0016$, $R^2=0.69$) (Fig. 2a), but the relation with mazindol urine concentration was not significant ($P=0.84$, $R^2=0.005$) (Fig. 2b). ΔBP in the caudate was significantly correlated with mazindol plasma concentration ($P=0.024$, $R^2=0.46$), but the relation with mazindol urine concentration was not significant ($P=0.40$, $R^2=0.079$). ΔBP in the putamen was significantly correlated with mazindol plasma concentration ($P=0.0063$, $R^2=0.58$), but the relation with mazindol urine concentration was not significant ($P=0.98$, $R^2=0.00$). Even with multiple comparisons using the Bonferroni correction, significant differences were observed in the putamen and caudate ($P<0.025=0.05/2$).

Discussion

This was the first study to investigate the effect of mazindol on the extracellular dopamine concentration in the striatum in healthy volunteers in vivo. Our study demonstrated that dopamine D_2 receptor binding in the striatum was decreased after taking mazindol (1.74 % with 0.5 mg and 8.14 % with 1.5 mg). Changes in dopamine D_2 receptor binding (ΔBP) with mazindol were significantly correlated with plasma concentration. We used [^{11}C]raclopride to estimate the changes in dopamine concentration in the striatum by assessing the changes in dopamine D_2 receptor bindings before and after taking mazindol. Of course, we could not directly evaluate the ability to synthesize dopamine and dopamine transporter function. However, it is possible that the BP decrease by mazindol in our study might have resulted from the inhibition of dopamine transporter, instead of an effect on dopamine release promoting action (Carruba et al. 1977; Parker and Cubeddu 1988).

From PET studies, drug-induced dopamine increase has been reported with other addictive drugs. Increased dopamine concentration evaluated by changes in BP_{ND} has been reported as follows: (1) oral administration of amphetamine at 0.5 mg/kg among healthy individuals decreased binding by 12.3 %; (2) intravenously-injected amphetamine at 0.3 mg/kg among healthy individuals decreased binding by 10.2 %; 3) Using gum containing nicotine at 2 mg among smokers decreased binding by 7.3 % (Takahashi et al. 2008; Narendran et al. 2010; Wand et al. 2007). We could not simply compare amphetamine and mazindol because their mechanisms of action are different, but 1.5 mg (0.02 mg/kg) of mazindol was comparable to between 0.3 mg/kg of amphetamine and 2 mg of nicotine with reference to the values of the above-mentioned literatures (Narendran et al. 2010; Wand et al. 2007). In fact, it has been reported that mazindol-induced hallucinations and a delusional state in an amphetamine-abuser (Kaneko et al. 2008). It was also reported that the administration of mazindol worsened the psychotic symptoms of schizophrenia (Krumholz and White 1970). Our findings suggested that the prescribed dose of mazindol might have the possibility to change the behavior and mental effects similarly to those of addictive amphetamine.

The other important finding in our study was that the change in the concentration of dopamine in the synaptic cleft was in a dose-dependent manner in vivo. This result was consistent with a previous study in rats, which reported an inhibitory effect on dopamine reuptake, and the increase in dopamine concentration by mazindol was dose-dependent (Carruba et al. 1977). Another study reported that the rewarding effects of drugs were associated with increases in brain dopamine concentration (Volkow et al. 2002). Our results that mazindol caused a dose-dependent increase in the concentration of dopamine in the striatum indicate that higher doses of mazindol might be more likely to cause dependence. Moreover, in both the caudate and putamen, dose-dependent increases in the concentration of dopamine were observed. The relationship between drug dependence and concentration change in dopamine with mazindol should be evaluated in more detail, including regional differences, using PET in the future.

It is well known that there are gender differences in the human dopamine system (Mozley et al. 2001). The correlation of ΔBP in the striatum and plasma concentration was significant at $P=0.0008$ in covariation with gender. However, the interaction of gender and plasma concentration was not significant at $P=0.675$. We therefore consider that gender would not affect the relationship of ΔBP and plasma concentration in this study.

In addition, it may be necessary to consider internalization. A previous animal study reported that the internalization of dopamine receptors was caused by psychostimulant (Skinbjerg et al. 2010). Although the details are not clear, the decrease of BP_{ND} in this study might be affected by this factor.

In conclusion, mazindol increased the concentration of dopamine in the synaptic cleft, and its effect was dose-dependent. A single administration of mazindol, even if at prescription dosage, elevated dopamine concentration comparable to other addictive drugs such as amphetamine and nicotine. It is suggested that the risk of dependence may increase with the dosage of mazindol.

Acknowledgments This work was partially supported by a grant from the Ministry of Education, Culture, Sports, Science and Technology (MEXT, Japan). We thank Minoru Sakurai, Koji Nagaya, Koji Kanaya, Masaya Suda, Megumi Takei, and Kazuyoshi Honjo (Clinical Imaging Centre for Healthcare, Nippon Medical School) for their assistance in performing MRI and PET examinations.